IEEE Access
Multidisciplinary | Rapid Review | Open Access Journal

Received September 18, 2018, accepted October 18, 2018, date of publication October 26, 2018,
date of current version November 30, 2018.

Digital Object Identifier 10.1109/ACCESS.2018.2878149

Temperature Rise for Brief Radio-Frequency Exposure Below 6 GHz

SACHIKO KODERA[1], AKIMASA HIRATA[1], (Fellow, IEEE), DAISUKE FUNAHASHI[1], SOICHI WATANABE[2], (Member, IEEE), KARI JOKELA[3], AND RODNEY J. CROFT[4]

[1]Department of Electrical and Mechanical Engineering, Nagoya Institute of Technology, Nagoya 466-8555 Japan
[2]EMC Group, Applied Electromagnetic Research Institute, National Institute of Information and Communications Technology, Tokyo 184-8795, Japan
[3]Ilmalankatu 6A7, 00240 Helsinki, Finland
[4]Australian Centre for Electromagnetic Bioeffects Research, Illawarra Health & Medical Research Institute, University of Wollongong, Wollongong, NSW 2522, Australia

Corresponding author: Akimasa Hirata (ahirata@nitech.ac.jp)

This work was supported by the Committee to Promote Research on the Possible Biological Effects of Electromagnetic Fields of the Ministry of Internal Affairs and Communications, Japan.

ABSTRACT In international guidelines for human protection from radio-frequency (RF) electromagnetic fields, the specific absorption rate (SAR) averaged over 6 min and 10 g of tissue is used as a physical quantity to prevent excess local temperature rise. The resultant SAR restriction has been set to avoid potential adverse health effects due to the temperature elevation resulting from RF energy absorption. In the public consultation version of the upcoming ICNIRP RF guidelines (July 10, 2018), a specific absorption (SA) limit was set to avoid heating from brief exposures (shorter than 6 min). However, to the best of our knowledge, no prior research has evaluated the temperature rise for single/multiple pulses with energy equivalent to the 6-min exposure SAR restriction for continuous waves. This paper computed the temperature rise for brief pulse exposures based on bioheat computations. We first confirmed that the peak temperature rise for a pulse with SA corresponding to occupational exposure exceeds the steady-state temperature rise for temporally uniform continuous wave exposure. We then proposed the SA limit from a regression curve that is dependent on the duration of brief exposure to RF pulse(s). The temperature rise in a multilayer cube and an anatomical human model were also computed for exposures to multiple pulses. The temperature rise from multiple pulses satisfying the formula was found to be below the relevant threshold level. The SA based on this regression curve can be used as a metric to prevent excess temperature rise for different brief exposure scenarios below 6 min.

INDEX TERMS Biological effects of radiation, dosimetry, product safety engineering, radiation safety, standardization.

I. INTRODUCTION

International standardization bodies use the specific absorption rate (SAR) as a physical quantity to prevent excess temperature rise due to radio-frequency (RF) exposure [1]–[3]. The SAR averaged over 10 g of tissue and whole-body averaged SAR are used as dose metrics, which are surrogates for local and core temperature rises respectively.

In current international standards, the averaging time for local exposure is 6 min for frequencies up to 3 GHz for controlled environments [2] or 10 GHz [1]. Recent studies discussed the effectiveness of this averaging time [4]. Unlike body-core temperature elevation, whose time constant is of the order of an hour or longer [5], the time required for local temperature to reach a steady state is the order of a few dozen minutes [6], [7] and depends on frequency and exposure area/volume [8].

If all the energy over an averaging time of 6 min was concentrated into a short duration (e.g., several seconds), the local temperature rise for a pulse may exceed that due to constant exposure [9]. This is because the effect of blood perfusion is marginal for brief exposures (e.g., several seconds), and thus the adiabatic condition is approximately valid. Indeed, the temperature rises almost linearly with time in such cases. The electromagnetic energy is thus concentrated on the superficial part of the 10 g-averaged SAR volume, which is due to the penetration depth decreasing as a function of frequency. Also, in adiabatic conditions the uneven distribution

of local SAR in conducting tissues such as skin, in contrast to low conducting fat, increases local peak temperature before the heat diffusion washes them out. Human protection for such pulses that are shorter than the averaging time has been discussed in e.g., Global Coordination of Research and Health Policy on RF Electromagnetic Fields (GLORE) in November 2017 (Washington DC, USA). Further analysis is therefore needed to understand the temperature rise due to brief intervals in order to protect humans for pulses that are shorter than the averaging time.

For frequencies above 10-30 GHz, the radiant exposure (incident energy density) averaged over a specific area is currently being discussed (e.g., GLORE in November 2017). This physical quantity is a good metric to describe skin temperature elevation, as it is supported by surface heating theory [10] and a computational model [11]. Note that, as is similar to continuous exposure, a physical quantity corresponding to local temperature elevation is "transmitted" energy density. The transmitted energy density is a new physical quantity introduced as the basic restriction above 6 GHz in the ICNIRP public consultation document. For brief exposure above 6 GHz, the correlation between the transmitted energy density and the temperature elevation is computed [12].

For frequencies below 6 GHz, the corresponding physical quantities would be specific (energy) absorption (SA) [2]. It was mentioned in the ICNIRP 1998 guidelines [1] that *"For frequencies exceeding 10 MHz, S_{eq}*(equivalent power density)*as averaged over the pulse width should not exceed 1,000 times the reference levels or that field strengths should not exceed 32 times the field strength reference levels. For frequencies between about 0.3 GHz and several GHz, and for localized exposure of the head, in order to limit or avoid auditory effects caused by thermoelastic expansion the specific absorption from pulses must*(be)*limited."* The IEEE C95.1 standard [2] mentioned that "*For short duration exposures the BRs*(basic restrictions)*and MPEs*(maximum permissible exposures)*are related to energy, i.e., specific absorption (SA) or energy density.*" In the ICNIRP public consultation document, the microwave hearing effect [13] caused by thermoelastic waves are not considered as an harmful tissue damaging effect. The SA is also used to limit temperature rise from brief pulses, but for a different purpose. Specifically, it was set to limit temperature rise to 5 and 2 °C for superficial and deeper tissue, respectively. The reduction factor 2 was applied for occupational exposure. The SA limit was mentioned in the IEEE C95.1 standard, and equivalently instantaneous peak power density is limited below a certain level.

However, to the best of our knowledge, no study has evaluated temperature rise for a pulse or pulse trains with energy concentrated shorter than the averaging time (6 min). Since it is difficult to measure absorbed energy and resultant temperature rise in tissue, we took the approach to evaluate this problem by deriving the computational relation. The purpose of the present study is to determine how best to set the metric in order to limit temperature rise from brief exposures at frequencies lower than 6 GHz.

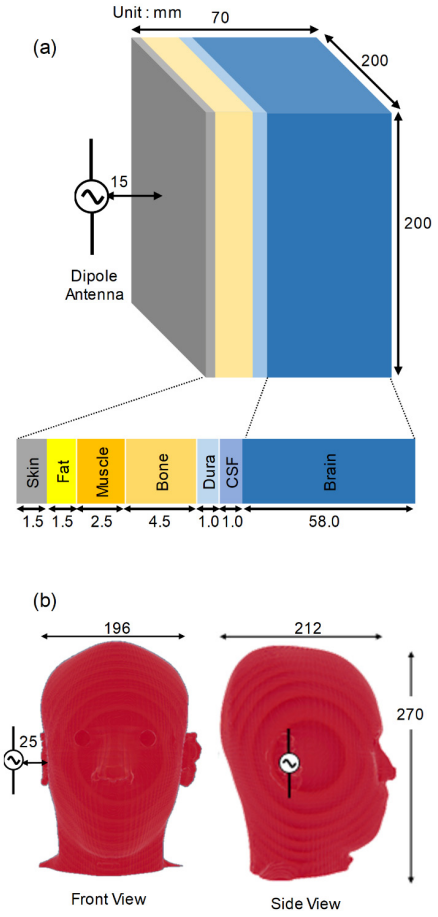

FIGURE 1. Exposure scenario with (a) a multilayer cube model and (b) an anatomical head model.

II. MODELS AND METHODS

A. NUMERICAL HEAD MODELS

Fig. 1 (a) shows a three-dimensional multilayer cube model that was used for simulating a human head. This model is comprised seven-layers; the skin (1.5 mm), fat (1.5 mm), muscle (2.5 mm), skull (4.5 mm), dura (1.0 mm), cerebrospinal fluid (1.0 mm), and brain (58.0 mm) [14]. In addition, a realistic anatomical model named TARO, which represents a Japanese adult male [15], was used for verifying the results from the cubic model, as shown in Fig. 1(b). The model with an original resolution of 2 mm was segmented into 51 anatomical regions. The model resolution was further divided into 0.5 mm cells to eliminate substantial computational error in finite-difference time-domain (FDTD) methods. The TARO was truncated at the bottom of the neck as we only discuss the exposure scenario in the head. The truncated head model is composed of 23 tissues.

B. ELECTROMAGNETIC ANALYSIS

The FDTD method [16], which has capability of handling inhomogeneous materials like biological bodies, was used

to conduct electromagnetic dosimetry in the human head models. The SAR was defined as

$$SAR(\mathbf{r}) = \frac{\sigma(\mathbf{r})}{2\rho(\mathbf{r})} |\mathbf{E}(\mathbf{r})|^2 , \quad (1)$$

where $|\mathbf{E}|$ is the peak value of the electric field at position r, and σ and ρ are the conductivity and mass density of the tissue, respectively. The dielectric properties of the tissues were determined with a Cole–Cole dispersion model [17].

As no averaging volume/mass has been discussed for the SA, 10 g averaging mass was chosen considering the continuity at the limit for longer than 6-min exposures. If this averaging mass was not used, the compliance may become very complicated; the evaluation metric varies with exposure duration. The SAR was averaged over 10 g of tissues in a cube shape following IEEE C95.3 [3], IEEE 1528-2013 [18], and IEC 62209-1:2016 [19]. In the current ICNIRP guidelines [1], the averaging volume of SAR corresponds to contiguous tissue, but has been changed to a cube in the ICNIRP public consultation document.

C. THERMAL ANALYSIS

The computational method for temperature elevation is identical to that in our previous study [20]. The temperature in the human model is computed by solving the Pennes's bioheat transfer equation (BHTE) [21]. This equation, which takes into account various heat exchange mechanisms such as conduction, blood perfusion, and electromagnetically induced heating, is represented by the following equation:

$$\begin{aligned} C(\mathbf{r})\rho(\mathbf{r})\frac{\partial T(\mathbf{r},t)}{\partial t} \\ = \nabla\left(K(\mathbf{r})\nabla T(\mathbf{r},t)\right) + \rho(\mathbf{r})SAR(\mathbf{r}) \\ + M(\mathbf{r},t) - B(\mathbf{r},t)\left(T(\mathbf{r},t) - T_B(t)\right), \end{aligned} \quad (2)$$

where T is temperature of the tissue, T_B is blood temperature, C is specific heat of the tissue, K is thermal conductivity of the tissue, M is metabolic heat generation, B is term associated with blood perfusion, and t is time. The blood temperature is assumed to be spatiotemporally constant in the same tissue because the exposure scenario considered here describes localized exposure. Hence, the blood temperature T_B(t) in (2) is treated as constant (37 °C). Metabolic heat generation was not considered in this study because it does not affect the steady state temperature elevation when the thermoregulatory response is ignored. The boundary condition between ambient air and tissue for (2) is given by

$$-K(\mathbf{r})\frac{\partial T(\mathbf{r},t)}{\partial n} = H\left(T_S(\mathbf{r},t) - T_e(t)\right), \quad (3)$$

where H, T_s, and T_e denote the heat transfer coefficient, surface temperature of the tissue, and ambient temperature (independent of position), respectively. The variable $n$denotes the axis perpendicular to the model surface. The BHTE was solved subject to the boundary condition in (3).

Table 1 shows the thermal parameters used in this study. The thermal parameters used in this study are the same as those used by [22], where the parameters were borrowed primarily from [23]. In addition, the blood perfusion rate through skin was the same as that used in [10]. The blood perfusion varies substantially even in a shallow region (surface to 3 mm). Its impact on the surface temperature rise is ±15% at frequency higher than 6 GHz [11], which is consistent with Monte-Calro approach by [24]. This study used relatively low blood perfusion rate to discuss conservative temperature rise in RF exposure safety. Note that for relatively brief exposure (e.g., < 10 s), the effect of the blood perfusion rate on the temperature rise is negligible. The heat transfer coefficient between skin and air was set to 5 W/m^2/°C, which is a typical value at an ambient temperature of 23 °C [25]. Thermoregulation, such as vasodilation and sweating, were not considered in this study as the exposure duration is brief and thus the temperature elevation is confined around the surface in most cases (e.g. [25], [26]).

TABLE 1. Thermal constant and mass density of human tissue

Tissues	K	C	B	M	ρ
Skin	0.42	3600	7367	1620	1125
Muscle	0.50	3800	2700	480	1047
Fat	0.25	3000	1626	300	916
Cortical Bone	0.37	3100	3400	610	1990
Cancellous Bone	0.41	3200	3300	530	1920
Cartilage	0.47	3600	9000	1600	1097
Nerve	0.46	3400	40000	7100	1038
Dura	0.50	3600	9100	0	1125
Gray Matter	0.57	3800	40000	7100	1038
White Matter	0.50	3500	40000	7100	1038
Cerebellum	0.57	3800	40000	7100	1038
CSF	0.62	4000	0	0	1007
Hypothalamus	0.57	3800	40000	7100	1038
Vitreous Humor	0.58	4000	0	0	1009
Lens	0.40	3000	0	0	1053
Retina	0.58	4000	0	0	1026
Blood	0.56	3900	0	0	1058
Tongue	0.54	3800	2700	480	1047
Thalamus	0.57	3800	40000	7100	1038
Pituitaria	0.57	3800	40000	7100	1038
Pineal	0.57	3800	40000	7100	1038
Trachea	0.47	3650	3700	1600	1100
Glandula Salivaria	0.42	3500	2350	4200	1000
Brain (Averaged)	0.57	3800	40000	7100	1038

The parameter of K (W/m/°C) is thermal conductivity of the tissue, C (J/kg/°C) is specific heat of the tissue, B (W/m^3/°C) is parameter of blood perfusion, M (W/m^3) is basal metabolism, ρ (kg/m^3) is density of tissue.

D. EXPOSURE SCENARIOS

Fig. 1 illustrates exposure scenarios using the multilayer cube model and the anatomical model in this study. The frequencies of the RF fields were 0.1, 0.3, 0.4, 0.5, 1, 3 and 6 GHz. To simulate plane-wave exposure using the multilayer cube, we conducted a 1D analysis with the same seven-tissue composite for simplicity. Hereafter, the 1D analysis will be referred to as plane wave exposure.

Considering the effect of field non-uniformity, a half-wave dipole antenna was also considered as a canonical near-field source. The length of the half-wave dipole antenna was adjusted to approximately half the wavelength of the RF field

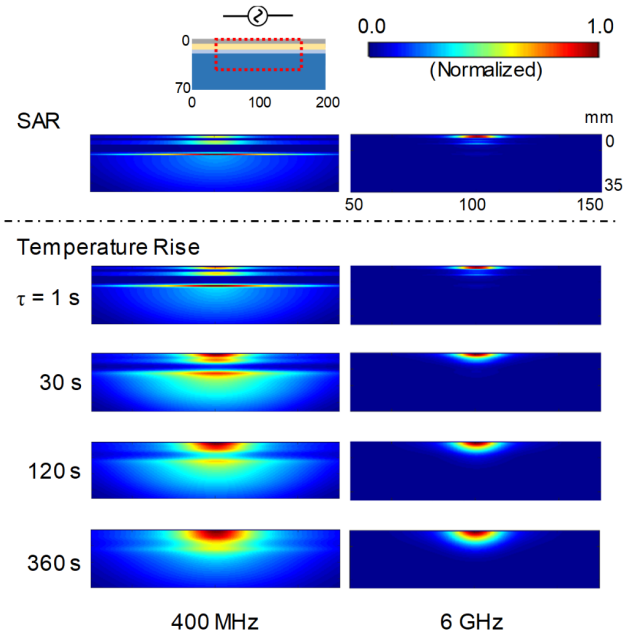

FIGURE 2. SAR distribution (adjusted to 10 g averaged peak SAR at 10 W/kg) and temperature rise (at constant specific absorption (SA) = 3.6 kJ) in the multilayer cube model. Distribution of temperature rise were normalized at the peak temperature rise in each scenario.

so as to resonate at the respective frequencies. The separation distances between the dipole antenna and the surface of the cube model and the head model were set to 15 mm and 25 mm, respectively.

III. COMPUTATIONAL RESULTS

A. TEMPERATURE RISE IN SKIN AT CONSTANT SA AND DIFFERENT FREQUENCIES

Fig. 2 shows the SAR distributions and temperature rise at 400 MHz and 6 GHz in the multilayer cube model for exposure from the dipole antenna. The distributions of temperature rise were obtained at constant SA (3.6 kJ/kg, corresponding to the energy of 10 W/kg for 6 min) and were normalized at the peak temperature rise in each scenario. Note that the basic restriction is 10 W/kg for occupational exposure, and the averaging time is set to 6 min below 3 GHz in IEEE C95.1 [2] and 10 GHz in ICNIRP [1]. As shown in Fig. 2, the temperature rise distributions for short exposure duration (e.g., 1 s) is almost identical to the SAR distributions, whereas it becomes smoother with increased time due to heat diffusion. The peak temperature rise at 400 MHz and 6 GHz were 2.5 and 9.8 °C for 1 s short exposure, while they became 0.9 and 2.0 °C at 6 min, respectively. These results suggest that an enhanced temperature rise can be observed at higher frequencies. The spatial peak temperature rise appeared in the skin (i.e., at the model surface) except at 3 GHz, which is attributable to the standing wave in the tissues.

Fig. 3 shows the peak temperature rise in a multilayer cube at constant SA (3.6 kJ/kg) for exposure to a dipole antenna and plane wave. For comparison, the steady-state temperature rise for 10 W/kg was also plotted. The temperature rise at 6 min is lower than that at the steady state because the time required to reach the steady state is longer than 6 min at frequencies below 6 GHz [4]. The temperature rise for the dipole antenna is not shown at 100 MHz because its dimension (approximately 150 cm) is much larger than that of the head size. Thus, results for the dipole antenna at 100 MHz may become similar to the results from plane wave exposure at 100 MHz just as their results at 300 MHz were similar.

As shown in Fig. 3, an energy concentration of less than 30 s below 500 MHz is required to induce a temperature rise larger than that of the steady state for plane wave exposure, but the exposure time is somewhat longer for a dipole antenna. This difference is attributable to the difference in SAR distribution (see Fig. 2). For short pulse duration at 6 GHz, a factor of 4 enhancement was observed. Also from Fig. 3, the effect of frequency on pulse-induced temperature elevation is dominant over the field distributions (dipole antenna versus plane wave). At the same frequencies, the difference was smaller than a factor of 2.

B. EFFECTIVENESS OF SA AS BASIC RESTRICTIONS

Fig. 4 summarizes the SA required for a skin temperature rise of 1 °C for different parameters; frequencies, sources, and exposure durations. Even at 1 s, the variability of temperature rise by SA is significant (see Fig. 3). For increasing frequency, the SA is concentrated on more superficial layers and consequently less absorbed energy is needed for the same temperature rise as at lower frequencies where the energy is distributed to a larger volume. For decreasing exposure durations, the decrease of heat flow has a similar effect on temperature rise. As shown in Fig. 4, the required SA decreases as the exposure duration decreases. The heat diffusion length depends on the exposure time, resulting in the SA difference required for a given temperature rise (see Fig. 2).

The draft of IEEE C95.1 limits skin temperature rise to 2-3 °C. The ICNIRP public consultation document applied a reduction factor of 2 to the 5 °C temperature elevation in tissues which typically have lower thermo-normal temperatures. The SAR averaged over 10 g tissue for localized exposure was set to 10 W/kg for occupational exposure according to the standards and guidelines available for RF protection at that time. This resulted in a steady-state temperature rise of approximately 2.5 °C at 0.1–6 GHz (see Fig. 3). In the following discussion, we chose 2.5 °C as a reference, and then the corresponding SA is discussed based on the bioheat calculation. This can be confirmed also by Fig. 2, which shows that the peak temperature rise occurs at skin rather than internal organs whose allowable temperature rise is 1 °C.

Fig. 5 shows the SA required for a temperature rise of 2.5 °C by rescaling Fig. 4 and the allowable SA (= 3.6 kJ/kg) for head and trunk tissue. The allowable SA at 6 min was designed to match SAR for the head and torso tissues (not in the limb) in a conservative manner. As shown in Fig. 4, the scenario resulting in the lowest SA required for a temperature rise of 2.5 °C is from the dipole antenna

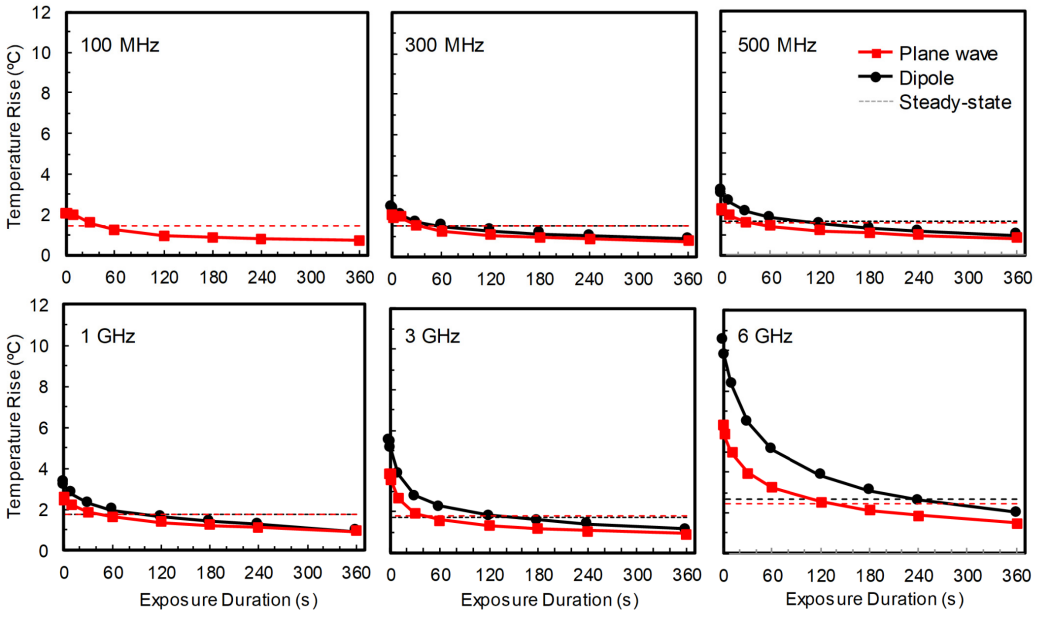

FIGURE 3. Temperature rise in multilayer cube model for dipole antenna and plane wave exposure. The SA was adjusted to 3.6 kJ/kg. The observed points correspond to the maximum temperature elevation. The steady-state temperature rise (duration longer than 30 min) are also plotted for comparison.

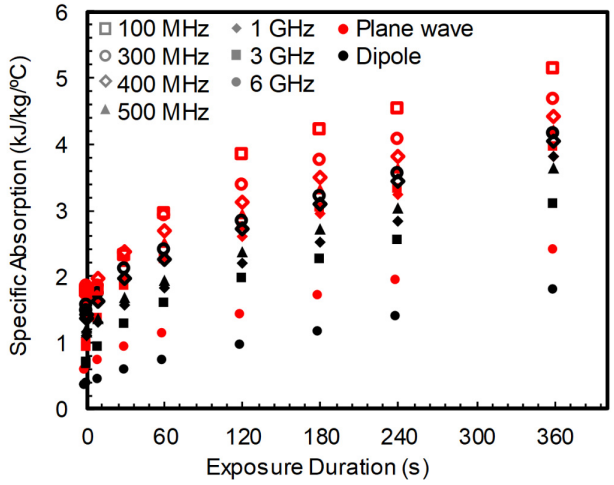

FIGURE 4. SA required for temperature elevation of 1 °C for exposure from dipole antenna and plane wave using multilayer cube model.

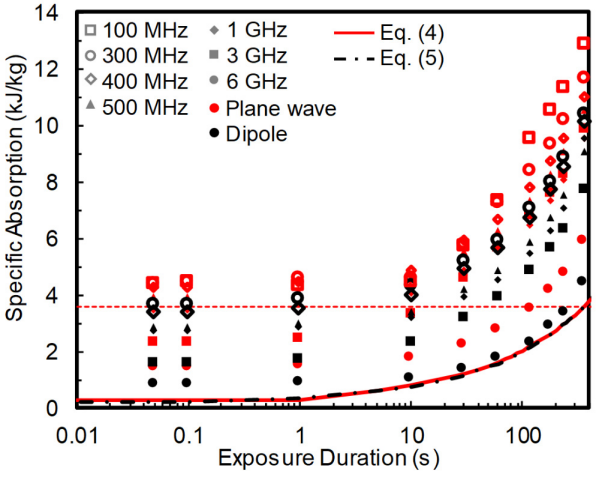

FIGURE 5. SA required for a temperature elevation of 2.5 °C. The allowable SA for occupational exposure and proposed regression curve are also plotted.

exposure at 6 GHz. This condition corresponds to a non-uniform SAR distribution in the averaging cube (10 g). The SA required below a few seconds of exposure is almost duration-independent, and then increases gradually as the exposure duration increases. The local temperature rise for a short-pulse ($\tau > 0.01$ s) with intense exposure of 3.6 kJ/kg exceeds 2.5 °C at frequencies higher than 500 MHz. We thus proposed a regression curve for the allowable SA to match 3.6 kJ/kg exposure at 6 min as follows:

$$SA = \begin{cases} 0.25 & \tau < 1 \text{ s}, \\ 0.25 + 0.177\sqrt{\tau - 1} & 1\text{s} \le \tau < 360 \text{ s}, \end{cases} \quad (4)$$

where τ denotes the RF exposure duration. For irregular pulse patterns or non-constant exposure levels, any exposure for exposure durations (“temporal analysis windows”) between the pulse duration and τ is considered, as is the same in the incoherent guidelines. Note that the regression curve is assumed to be proportional to the square root of duration with an intercept below 1 s, which is approximately chosen as adiabatic regime of temperature elevation. The function form is based on the analytic solution by [10].

Another expression for the regression curve is chosen as follows considering allowable SA at 6 min as well as the adiabatic conditions:

$$SA = 3.6\left(0.05 + 0.95\sqrt{t/360}\right), \quad (5)$$

The proposed regression curves in (4) and (5) are plotted in Fig. 5, which almost coincide each other.

C. DEMONSTRATIONS FOR MULTIPLE PULSES

We computed the following four scenarios to confirm the change in temperature over time: i) five different short pulses of 0.1 s exposure; ii) continuous exposure to a 0.1 s pulse with intervals of 2 s, iii) after exposure of a continuous wave for 30 min, followed by a 6 min pause and a 1 s pulse exposure; iv) four repetitions of 200 s pulses and 160 s pauses. The SA values in all scenarios were adjusted so as not to violate the regression curve in (4). Note that (5) is more conservative than (4) except around 1 sec, and thus (4) is used in the remaining of the study. The exposure scenarios (iii) and (iv) considered more than 6 min to confirm the cumulative effect of temperature rise in possible complicated environments.

Fig. 6 shows the time dependence of the subjected peak SAR averaged over 10 g of tissue and the resulting temperature rise at the position where the peak temperature appeared in the multilayer cube model in exposure scenarios (i), (ii), (iii), and (iv). To clearly show the effect of temperature for exposure to multiple pulses, the peak temperature was normalized at the peak steady-state temperature rise for continuous exposure (adjusted to 10 g averaged peak SAR at 10 W/kg). As shown in Fig. 6, the temperature rise for exposure to multiple pulses was below the steady-state temperature in most investigated cases. In the case of Fig. 6d, the instantaneous peak temperature rise reached 2.3% above the steady state temperature rise. The peak temperature rise did not exceed the steady-state temperature when the separation distance between the dipole antenna and the surface of the cube model was set to 25 mm in the same scenario. Fig. 7 shows the temperature rise in skin and brain tissue at 400 MHz in exposure scenarios (iii) and (iv). The peak temperature rise in the brain was 0.82 °C for continuous exposure adjusted to 10 g averaged peak SAR at 10 W/kg for 6 min. The normalized temperature rise in the brain was 95% and 89% of steady-state temperature in Figs. 7a and 7b, respectively. The brain temperature elevates higher at lower frequencies because the penetration depth of electromagnetic field is deeper than at higher frequencies. The computed SAs below 3 GHz are sufficiently higher than the regression curve in Fig. 5. Thus, the regression curve also suppressed the brain temperature rise for exposure to multiple pulses.

In addition, we computed the temperature rise using the anatomical head model in several scenarios. Fig. 8 shows the temperature rise in the anatomical head model in exposure scenarios (i), (iii), and (iv). The peak temperature for exposure to multiple pulses was normalized at the peak steady-state temperature rise for continuous exposure (adjusted to 10 g averaged peak SAR at 10 W/kg), as in the case of the multilayer cube model. As shown in Fig. 8a–d, the peak temperature rise for multiple pulses in the human head was less than 98% of the steady-state temperature rise. The normalized temperature rise of the anatomical model was lower than that of the multilayer model.

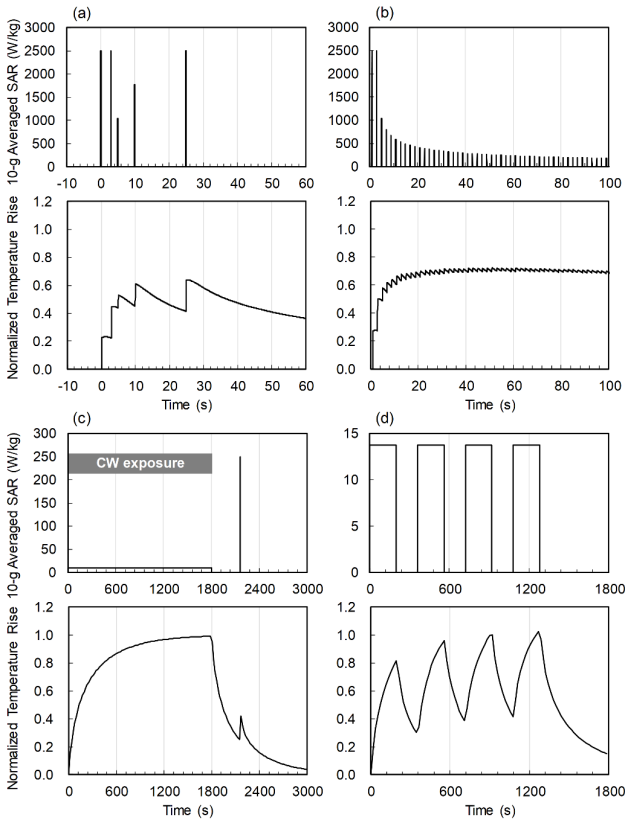

FIGURE 6. Time dependence of the peak SAR averaged over 10 g of tissue, and the resulting temperature rise for exposure to multiple pulses from a dipole antenna using the TARO head model. The frequencies are (a, b) 6 GHz and (c, d) 1 GHz. The temperature rise in the brain are also plotted for exposure to a dipole antenna at 1 GHz. The SAR averaged over 10 g was adjusted so that the SA did not exceed the proposed regression curve. The temperature was normalized at the peak steady-state temperature rise for continuous exposure (adjusted to 10 g averaged peak SAR at 10 W/kg).

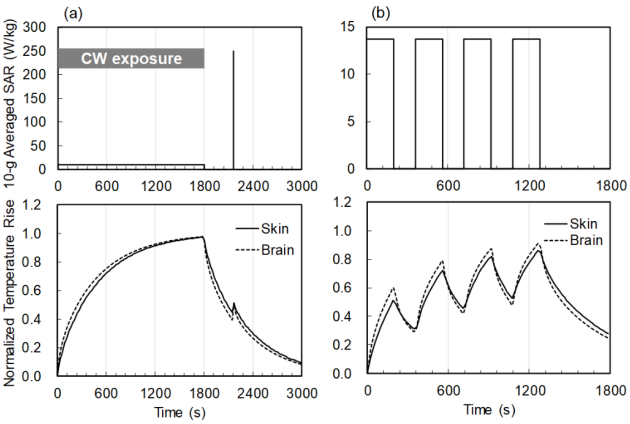

FIGURE 7. Time dependence of the peak SAR averaged over 10 g of tissue and the resulting temperature rise for four scenarios of multiple pulse exposure from a dipole antenna at 6 GHz using the multilayer cubic model. The SAR averaged over 10 g was adjusted so that the SA did not exceed the proposed regression curve. The temperature was normalized at the peak steady-state temperature rise for continuous exposure (adjusted to 10 g averaged peak SAR at 10 W/kg).

IV. DISCUSSION

We computed the temperature rise for pulse exposures using the multilayer cubic and anatomical human models. The main

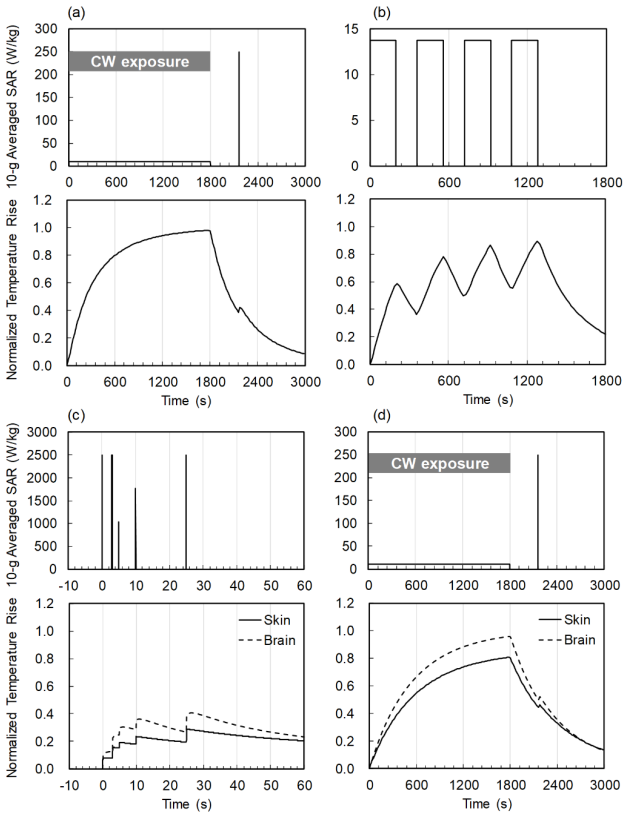

FIGURE 8. **The time dependence of the peak SAR averaged over 10 g of tissue and the resulting temperature rise in skin and brain using the multilayer cubic model for exposure to multiple 400 MHz pulses from a dipole antenna. The SAR averaged over 10 g was adjusted so that the SA did not exceed the proposed regression curve. The temperature was normalized at the peak steady-state temperature rise for continuous exposure (adjusted to 10 g averaged peak SAR at 10 W/kg).**

contribution of this study was to reveal the limitation of SA in the current guidelines for pulse exposures and to propose a new limit.

The definition of the basic restriction in the ICNIRP 1998 guidelines [1] states "*Restrictions on exposure to time-varying electric, magnetic, and electromagnetic fields that are based directly on established health effects are termed "basic restrictions". Depending upon the frequency of the field, the physical quantities used to specify these restrictions are current density (J), specific energy absorption rate (SAR), and power density (S).*" Repetitive exposure (i.e., repetitive pulses, intermittent exposure, or non-constant exposure) is stated in ICNIRP 2013 guidelines [27] *"As a basic principle, any exposure within the anticipated maximum exposure duration, has to be below the corresponding exposure limit for that duration."*

At RF frequencies below 6 GHz, the SAR averaged over 10 g of tissue and the entire body are used as physical quantities describing basic exposure restrictions for local and whole-body exposures. The 10 g averaged SAR has been demonstrated to be the one which can relate to a local temperature elevation. Although the SAR averaged over 10 g of tissue at a fixed temperature rise depends on local heat diffusion e.g., blood flow, the heating factor, which is the ratio of temperature rise to SAR is rather frequency independent [20]. Consequently, the steady-state temperature rise can be estimated once the SAR is obtained. The whole-body averaged SAR is also a good surrogate for steady-state body-core temperature rise, even though it depends on the sweating capability and body surface area-to-mass ratio, core temperature elevation can be estimated once the whole-body averaged SAR is obtained [28], [29].

There is, however, no clear trend between SA and local temperature rise. The difference between SA and SAR is that the temperature rise for SAR considers the steady state, whereas the temperature rise for SA is an instantaneous peak temperature rise. The distance that heat can diffuse then differs for different exposure durations. If the adiabatic condition is considered for uniform SAR distribution, the temperature rise at 1 s should be 1.06 °C from the SA (3.6 kJ/kg) and the specific heat (3400 J/kg/°C). The computed temperature rise was higher than this value but gradually came close to this value with decreased frequency. This is because of the non-uniformity in the SAR distribution, even in the averaging cube.

Fig. 3 shows that the temperature rise in the skin does not reach 2.5 °C at frequencies below 300 MHz, although it depends on the choice of the thermal parameters. An energy concentration shorter than 240 s induced a temperature rise larger than that of the steady state at 6 GHz, and the enhancement decreased as frequency decreased. The enhancement at 100 MHz is at most 40% and may be in the range of computational variability originating from the thermal parameters, the antenna position, and source modeling [30].

From the computational results, we derive a regression curves of SA to limit time-dependent allowable energy. The curves were designed considering the continuity with exposures longer than 6 min. The averaging time of 6 min has been prescribed in the international guidelines/standard for constant exposures. This value is supported by computational studies for local exposures [4], [6], [7]. In addition, the averaging mass for the SA was considered to match that of SAR. This is approximately the optimal mass to correlate the local SAR and local temperature elevations for constant exposure [29], [31]–[34]. If the latter were not specified, the compliance may become very complicated; the evaluation metric varies with time, as mentioned above. We chose the plane wave and the dipole antenna as canonical far-field and near-field wave source, respectively. Though not shown here to avoid repetition, we also computed the relationship between SA and temperature rise for a planar inverted-F antenna, which is used in a commercial wireless devices. We confirmed that the results of PIFA was in the range between the plane wave and the dipole antenna. For example, the SA required for a temperature elevation of 2.5 °C for exposure from PIFA was 2.48 kJ/kg/°C, which is 17% larger than the result of dipole and 4% smaller than the plane wave at 2 GHz.

We have computed the temperature rise over time in the skin and brain for multiple pulses when the SA did not exceed

the proposed regression curve in (4). The time-function form of the regression curve should match that above and below 6 GHz, considering exposure scenarios with frequency components both above and below 6 GHz. Equations below 6 GHz include an adjustment that incorporates the more conservative nature of the derivations for exposures above 6 GHz (see ICNIRP public consultation document).

We treated the peak temperature for multiple pulses normalized by the steady-state temperature corresponding to the peak SAR averaged over 10 g of tissue at 10 W/kg. This was performed because the peak SAR averaged over 10 g of tissue is used as the local exposure limit. As a result, the proposed regression curve kept the temperature rise below a given level for exposure to multiple pulses and below the steady-state temperature except for one exposure scenario investigated. The temperature rise from multiple pulses may exceed 10% or less above the steady state temperature rise, but that excess is within the range of numerical uncertainty discussed in IEEE ICES Technical Committee 95. One of the reasons of this exceedance is attributable to the temperature decay which is attributable to the non-uniformity of the specific heat in realistic models.

The SA may be applicable for realistic exposure assessment based on reference levels for external field strength or incident power density in the case of relatively uniform field such as generated by scanning high power radar antennas. The SA derived here is used for deriving the reference level by using the conventional relationship between SAR and external field strength [35]. The purpose of this limit is more related to the exposure of 10 sec or shorter. Practically, the SA may be applied for protection in occupational exposure where the intensity is higher than the limit for constant waves, but the exposure duration is shorter than 6 min. For example, pulses from radar antennas are assumed; 0.3 s pulses with intervals of 2 s at 3 GHz. The allowable energy per pulse restricted by the proposed curve decreases as the pulse repetition increases; it may match the limit for an averaging time of 6 min.

V. CONCLUSION

This study discussed the limit for human protection from brief RF exposures (the duration is shorter than 6 minutes) at frequencies lower than 6 GHz. There is no clear trend between SA and local temperature, unlike the relation between SAR averaged over 10 g of tissue and peak steady-state temperature rise. For brief exposures above 400 MHz, the maximum temperature rise at the SA corresponding to that from a 6 min local basic exceeds the steady state temperature, depending on the exposure scenario. Duration time dependence is more important to introduce new SA restriction. We proposed the SA based on the regression curve required for temperature elevation of 2.5 °C. In addition, we computed the temperature rise over time for four typical scenarios with exposure to multiple pulses in the multilayer cube and human anatomical models. The regression curve derived here would be a useful index to suppress tissue temperature rise from brief exposures. Further research may be required to explore a better physical quantity to relate the temperature rise for such exposures.

REFERENCES

[1] A. Ahlbom *et. al*, "Guidelines for limiting exposure to time-varying electric, magnetic, and electromagnetic fields (up to 300 GHz)," *Health Phys.*, vol. 74, no. 4, pp. 494–521, 1998.
[2] *IEEE Standard for Safety Levels With Respect to Human Exposure to Radio Frequency Electromagnetic Fields, 3 kHz to 300 GHz*, IEEE Standard C95.1-2005, 2006.
[3] *IEEE Recommended Practice for Measurements and Computations of Radio Frequency Electromagnetic Fields With Respect to Human Exposure to Such Fields, 100 kHz-300 GHz*, IEEE Standard C95.3-2002, 2002.
[4] R. Morimoto, A. Hirata, I. Laakso, M. C. Ziskin, and K. R. Foster, "Time constants for temperature elevation in human models exposed to dipole antennas and beams in the frequency range from 1 to 30 GHz," *Phys. Med. Biol.*, vol. 62, no. 5, pp. 1676–1699, 2017.
[5] A. Hirata, T. Asano, and O. Fujiwara, "FDTD analysis of human body-core temperature elevation due to RF far-field energy prescribed in the ICNIRP guidelines," *Phys. Med. Biol.*, vol. 52, no. 16, pp. 5013–5023, 2007.
[6] J. Wang and O. Fujiwara, "FDTD computation of temperature rise in the human head for portable telephones," *IEEE Trans. Microw. Theory Techn.*, vol. 47, no. 8, pp. 1528–1534, Aug. 1999.
[7] G. M. J. Van Leeuwen, J. J. W. Lagendijk, B. J. A. M. Van Leersum, A. P. M. Zwamborn, S. N. Hornsleth, and A. N. T. J. Kotte, "Calculation of change in brain temperatures due to exposure to a mobile phone," *Phys. Med. Biol.*, vol. 44, no. 10, pp. 2367–2379, 1999.
[8] Y. Hashimoto *et al.*, "On the averaging area for incident power density for human exposure limits at frequencies over 6 GHz," *Phys. Med. Biol.*, vol. 62, no. 8, pp. 3124–3138, Feb. 2017.
[9] K. R. Foster, A. Lozano-Nieto, P. J. Riu, and T. S. Ely, "Heating of tissues by microwaves: A model analysis," *Bioelectromagnetics*, vol. 19, no. 7, pp. 420–428, 1998.
[10] K. R. Foster, M. C. Ziskin, and Q. Balzano, "Thermal response of human skin to microwave energy: A critical review," *Health Phys.*, vol. 111, no. 6, pp. 528–541, Dec. 2016.
[11] I. Laakso, R. Morimoto, J. Heinonen, K. Jokela, and A. Hirata, "Human exposure to pulsed fields in the frequency range from 6 to 100 GHz," *Phys. Med. Biol.*, vol. 62, no. 17, pp. 6980–6992, 2017.
[12] A. Hirata, D. Funahashi, and S. Kodera, "Setting exposure guidelines and product safety standards for radio-frequency exposure at frequencies above 6 GHz: Brief review," *Ann. Telecommun.*, to be published.
[13] C.-K. Chou, A. W. Guy, and R. Galambos, "Auditory perception of radio-frequency electromagnetic fields," *J. Acoust. Soc. Amer.*, vol. 71, no. 6, pp. 1321–1334, 1982.
[14] A. Drossos, V. Santomaa, and N. Kuster, "The dependence of electromagnetic energy absorption upon human head tissue composition in the frequency range of 300-3000 MHz," *IEEE Trans. Microw. Theory Techn.*, vol. 48, no. 11, pp. 1988–1995, Nov. 2000.
[15] T. Nagaoka *et al.*, "Development of realistic high-resolution whole-body voxel models of Japanese adult males and females of average height and weight, and application of models to radio-frequency electromagnetic-field dosimetry," *Phys. Med. Biol.*, vol. 49, no. 1, pp. 1–15, 2004.
[16] A. Taflove and S. C. Hagness, *Computational Electrodynamics: The Finite-Difference Time-Domain Method*, 3rd ed. Norwood, MA, USA: Artech House, 2005.
[17] S. Gabriel, R. W. Lau, and C. Gabriel, "The dielectric properties of biological tissues: III. Parametric models for the dielectric spectrum of tissues," *Phys. Med. Biol.*, vol. 41, no. 11, p. 2271, 1996.
[18] *IEEE Recommended Practice for Determining the Peak Spatial-Average Specific Absorption Rate (SAR) in the Human Head From Wireless Communications Devices: Measurement Techniques*, IEEE Standard 1528-2013, 2013.
[19] *Measurement Procedure for the Assessment of Specific Absorption Rate of Human Exposure to Radio Frequency Fields From Hand-Held and Body-Mounted Wireless Communication Devices—Part 1: Devices Used Next to the Ear (Frequency Range of 300 MHz to 6 GHz)*, Standard IEC 62209-1:2016, 2016.
[20] R. Morimoto, I. Laakso, V. De Santis, and A. Hirata, "Relationship between peak spatial-averaged specific absorption rate and peak temperature elevation in human head in frequency range of 1–30 GHz," *Phys. Med. Biol.*, vol. 61, no. 14, pp. 5406–5425, 2016.

[21] H. H. Pennes, "Analysis of tissue and arterial blood temperatures in the resting human forearm," *J. Appl. Physiol.*, vol. 1, no. 2, pp. 93–122, 1948.
[22] A. Hirata, O. Fujiwara, and T. Shiozawa, "Correlation between peak spatial-average SAR and temperature increase due to antennas attached to human trunk," *IEEE Trans. Biomed. Eng.*, vol. 53, no. 8, pp. 1658–1664, Aug. 2006.
[23] F. Duck, *Physical Properties of Tissues: A Comprehensive Reference Book*. New York, NY, USA: Academic, 1990.
[24] K. Sasaki, M. Mizuno, K. Wake, and S. Watanabe, "Monte Carlo simulations of skin exposure to electromagnetic field from 10 GHz to 1 THz," *Phys. Med. Biol.*, vol. 62, no. 17, pp. 6993–7010, 2017.
[25] D. Fiala, K. J. Lomas, and M. Stohrer, "Computer prediction of human thermoregulatory and temperature responses to a wide range of environmental conditions," *Int. J. Biometeorol.*, vol. 45, pp. 143–159, Sep. 2001.
[26] S. Kodera, J. Gomez-Tames, and A. Hirata, "Temperature elevation in the human brain and skin with thermoregulation during exposure to RF energy," *Biomed. Eng. Online*, vol. 17, no. 1, pp. 1–17, 2018.
[27] International Commission on Non-ionizing Radiation Protection (ICNIRP), "ICNIRP guidelines on limits of exposure to incoherent visible and infrared radiation," *Health Phys.*, vol. 105, no. 1, pp. 74–96, 2013.
[28] A. Hirata, H. Sugiyama, and O. Fujiwara, "Estimation of core temperature elevation in humans and animals for whole-body averaged SAR," *Prog. Electromagn. Res.*, vol. 99, pp. 53–70, 2009.
[29] A. Hirata, I. Laakso, T. Oizumi, R. Hanatani, K. H. Chan, and J. Wiart, "The relationship between specific absorption rate and temperature elevation in anatomically based human body models for plane wave exposure from 30 MHz to 6 GHz," *Phys. Med. Biol.*, vol. 58, no. 4, pp. 903–921, 2013.
[30] I. Laakso, R. Morimoto, A. Hirata, and T. Onishi, "Computational dosimetry of the human head exposed to near-field microwaves using measured blood flow," *IEEE Trans. Electromagn. Compat.*, vol. 59, no. 2, pp. 739–746, Apr. 2017.
[31] A. Hirata and O. Fujiwara, "The correlation between mass-averaged SAR and temperature elevation in the human head model exposed to RF near-fields from 1 to 6 GHz," *Phys. Med. Biol.*, vol. 54, no. 23, pp. 7227–7238, 2009.
[32] R. L. Mcintosh and V. Anderson, "SAR versus VAR, and the size and shape that provide the most appropriate RF exposure metric in the range of 0.5–6 GHz," *Bioelectromagnetics*, vol. 32, no. 4, pp. 312–321, 2011.
[33] A. Razmadze, L. Shoshiashvili, D. Kakulia, R. Zaridze, G. Bit-Babik, and A. Faraone, "Influence of specific absorption rate averaging schemes on correlation between mass-averaged specific absorption rate and temperature rise," *Electromagnetics*, vol. 29, no. 1, pp. 77–90, 2009.
[34] J. F. Bakker, M. M. Paulides, E. Neufeld, A. Christ, N. Kuster, and G. C. van Rhoon, "Children and adults exposed to electromagnetic fields at the ICNIRP reference levels: Theoretical assessment of the induced peak temperature increase," *Phys. Med. Biol*, vol. 56, no. 15, pp. 4967–4989, 2011.
[35] G. Neubauer, P. Preiner, S. Cecil, N. Mitrevski, J. Gonter, and H. Garn, "The relation between the specific absorption rate and electromagnetic field intensity for heterogeneous exposure conditions at mobile communications frequencies," *Bioelectromagnetics*, vol. 30, no. 8, pp. 651–662, 2009.

SACHIKO KODERA received the B.E. and M.E. degrees in electrical and computer engineering from the Nagoya Institute of Technology, Nagoya, Japan, in 2002 and 2006, respectively.

In 2016, she joined the Department of Electrical and Mechanical Engineering, Nagoya Institute of Technology, as a Researcher. Her current research interests include electromagnetic and thermal dosimetry modeling in humans for radio-frequency and ambient heat exposures.

AKIMASA HIRATA (S'98–M'01–SM'10–F'17) received the B.E., M.E., and Ph.D. degrees in communications engineering from Osaka University, Suita, Japan, in 1996, 1998, and 2000, respectively.

From 1999 to 2001, he was a Research Fellow of the Japan Society for the Promotion of Science and also a Visiting Research Scientist with the University of Victoria, Victoria, BC, Canada, in 2000. In 2001, he joined the Department of Communications Engineering, Osaka University, as an Assistant Professor. In 2004, he joined the Department of Computer Science and Engineering, Nagoya Institute of Technology, as an Associate Professor, where he is currently a Full Professor. His research interests include electromagnetics and thermodynamics in biological tissue, waveguide analysis, EMC and EMI, and computational techniques in electromagnetics.

Dr. Hirata is a fellow of Institute of Physics, a Senior Member of IEICE and IEE Japan, and a member of Bioelectromagnetics Society. He is also an Editorial Board Member of physics in medicine and biology and a member of the main commission and the administrative committee. He received several awards, including the Young Scientists' Prize in 2006 and Prizes for Science and Technology (Research Category 2011, Public Understanding Promotion Category 2014) by the Commendation for Science and Technology from the Minister of Education, Culture, Sports, Science, and Technology, Japan, the IEEE EMC-S Technical Achievement Award in 2015, and the Japan Academy Medal in 2018. He is the Chair of project group of International Commission on Non-Ionizing Radiation Protection, the Subcommittee (EMF Dosimetry Modeling) Chair of IEEE International Committee on Electromagnetic Safety, and an Expert of the World Health Organization. From 2006 to 2012, he was an Associate Editor of the IEEE Transactions on Biomedical Engineering.

DAISUKE FUNAHASHI received the B.E. degree in electrical and electronic engineering from the Nagoya Institute of Technology, Nagoya, Japan, in 2017, where he is currently pursuing the master's degree in electrical and mechanical engineering.

His current research focuses on human protection from electromagnetic field at radio frequency.

SOICHI WATANABE (S'93–M'96) received the B.E., M.E., and D.E. degrees in electrical engineering from Tokyo Metropolitan University, Tokyo, Japan, in 1991, 1993, and 1996, respectively.

He is currently with the National Institute of Information and Communications Technology, Tokyo. His main research interests include biomedical electromagnetic compatibility.

Dr. Watanabe is a member of the Institute of Electronics, Information and Communication Engineers (IEICE), the Institute of Electrical Engineers, Japan, and the Bioelectromagnetics Society. From 2004 to 2012, he was a member of the Standing Committee III on Physics and Engineering of International Commission on Non-Ionizing Radiation Protection and has been a member of the main commission of ICNIRP since 2012. He received the 1996 Young Scientist Award from the International Scientific Radio Union, the 1997 Best Paper Award from IEICE, and the 2004 Best Paper Award (The Roberts Prize) of Physics in Medicine and Biology.

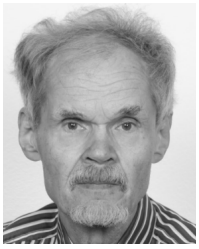

KARI JOKELA was born in Helsinki, Finland, in 1949. He received the Ph.D. degree in technology from the Helsinki University of Technology (Aalto University) in 1982.

From 1977 to 2015, he was with the STUK, Radiation and Nuclear Safety Authority, Finland, from 1992 to 2011 as the Head of the Non-Ionizing Radiation Laboratory and from 1997 to 2015 as a Research Professor. His main duties consisted of research, regulatory activities, management, and public information. He is the author or co-author of numerous scientific publications dealing mainly with microwave techniques, EM measurements, EM dosimetry, EM field protection standards, UV radiometry, and solar UV climatology.

Dr. Jokela has also been teaching at the Helsinki University of Technology, lecturing a course on NIR protection, and is the co-editor of the text book *Electromagnetic Fields* (STUK, Finnish). He has been serving ICNIRP first as a member of scientific standing committee SCIII since 1994 and then as a Commission Member from 2008 to 2016. He is currently a member of the Scientific Expert Group on PGHF guidelines that prepares new guidelines for RF fields from 100 kHz to 300 GHz.

RODNEY J. CROFT received degrees in philosophy and psychology, and the Ph.D. degree from the University of Wollongong, Australia, in 2000, where he developed methods for accounting for ocular artefact in the electroencephalograph.

He then worked in the area of cognitive neuroscience as a Post-Doctoral Researcher at Imperial College, London, and Swinburne University, Australia. He is currently a Professor of health psychology with the School of Psychology, University of Wollongong. His current research interests focus on the delineation of human brain function, particularly as it relates to agents that might affect it (e.g., electromagnetic fields, illicit, and medicinal drugs), as well as psychiatry more generally. He has been involved in research on extremely low frequency and radio frequency (RF) non-ionising radiation since 2000, primarily utilizing the electroencephalogram as a means of observing subtle alterations in brain function, but his research also encompasses epidemiological investigations of RF-cognition relations, RF-sleep research and RF-induced cell permeation, as well as radiation risk perception and communication more generally.

Dr. Croft is a Commissioner with the International Commission on Non-Ionizing Radiation Protection (ICNIRP). He chairs the ICNIRP revision of its upcoming RF guidelines. He was the Director of the Australian Centre for RF Bioeffects Research from 2004 to 2011 and the Australian Centre for Electromagnetic Bioeffects Research from 2013 to 2018.